J. Fluid Mech. (1993), *vol.* 255, *pp.* 621–646

Turbulent fountains in a closed chamber

By W. D. BAINES, A. F. CORRIVEAU AND T. J. REEDMAN
Department of Mechanical Engineering, University of Toronto, Toronto, ON, M5S 1A4, Canada

(Received 21 October 1991 and in revised form 30 April 1993)

An experimental and numerical investigation of the density distribution produced in a container by a negatively buoyant jet has been undertaken to evaluate the effect of the forced vertical motion of the environment. Vertical motion results from inflows and exhausts above and below the jet. Three distinct cases were identified. In the first, a velocity in the environment opposed the jet and produced a steady flow. This configuration was used to measure the entrainment flux along the length of the fountain. This configuration is similar to a jet impinging on an interface for which the entrainment depends on the local Froude number. The experiments covered a wider range of local Froude numbers than previously published and have produced results which are different from those in the literature. In the second case, the environment was at rest except for the motion induced by the fountain. An interface formed at the base of the fountain and moved quickly to the top. Once there, it advanced slowly due to entrainment through the end of the fountain and the length of the fountain increased. The final case is a co-flowing environment. No interface formed if the environment velocity was greater than the advance velocity of the end of the fountain. However, one formed for a smaller environment velocity and the end of the fountain was observed to undergo a quasi-periodic jump phenomenon. The top of the fountain would advance with the environment particles for a short time and then snap back to the elevation of a fountain in an infinite environment. A new interface formed and the cycle repeated.

1. Introduction

Negatively buoyant jets, referred to as fountains, are often encountered in both industry and nature. In any process where a heavy fluid is injected upward into a miscible lighter fluid a fountain forms. The heavy fluid penetrates to a finite height, stops and then flows back around the upward flow. The same flow is seen for a light fluid injected downward into a heavy one but in this paper the first case will be the sense of the discussion. The density difference may be due to a variation in either chemical composition or temperature but only the salt concentration was varied in these experiments. In this paper we are concerned with the interaction between the fountain and the environment. Focus is on the environment velocity, temperature and density profiles. This is an expansion of studies reported in the literature which have used either an infinite environment or an open container. In the latter, there is neither an inflow nor an exhaust in the zone occupied by the fountain. All of the flow from the source eventually passes above the elevation of the top of the fountain. In this paper we present the results of an experimental study designed to address the general case of an imposed vertical velocity in the environment. Figure 1 is a definition sketch of the geometry whereon the principle variables are defined. The results should be useful for a larger variety of practical problems.

Fountains are found in many applications in engineering and natural science. Ventilation problems, for example, typically involve heating or cooling of air and as a

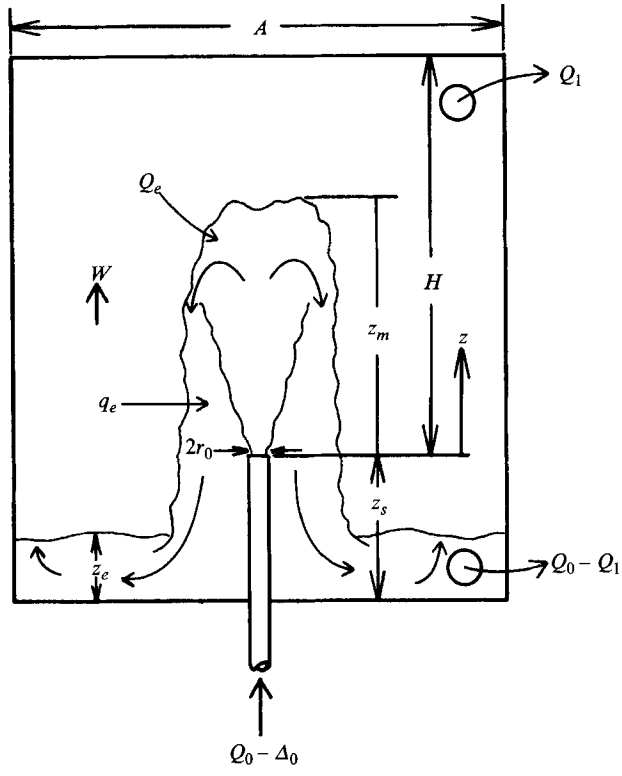

FIGURE 1. Definition sketch of a fountain in a container.

result buoyancy forces are produced. Heating of a large open structure, such as an aircraft hanger, by large fan-driven heaters at the ceiling level is one case sketched in figure 2(*a*). A hot jet must be produced with sufficient momentum to carry it through the cold air to the floor level. The resulting flow pattern is an inverted fountain as the mixed air rises up to the ceiling. The magma chamber of a volcano is an illustration of a fountain having buoyancy forces primarily due to differences in chemical composition. Dense magma is injected into an expanding chamber of lighter rock. Other flow patterns may not be so easily recognized as fountain driven. One such case is the mixing of a two-layer water reservoir with propellers. Figure 2(*b*) shows a water reservoir with a layer of cold water on the bottom. A propeller drives a jet of lighter fluid into the denser layer and the fountain is produced in the lower layer. The outflow spreads along the colder side of the interface between the warm and colder water. The lower layer is identical to the magma chamber or the aircraft hanger except for one small point; its volume increases steadily from the input of mixed fluid. The same layered flow pattern is found in metallurgical furnaces which are mixed by gas bubble plumes. Heavy fluid is driven upward by the rising bubbles and then falls back to the bottom of the lighter layer.

If the momentum in the jet is large enough, the fountain impinges on the opposite side of the enclosure. Here it spreads laterally before falling back around the upward flow. It is found that the entrainment into the fountain is significantly larger than for a fountain with a free end. Both the free and impinging cases are considered in this paper.

Several papers are relevant to the present study. Morton (1959) analysed a fountain as one case of a forced plume. This solution, which was based on a constant

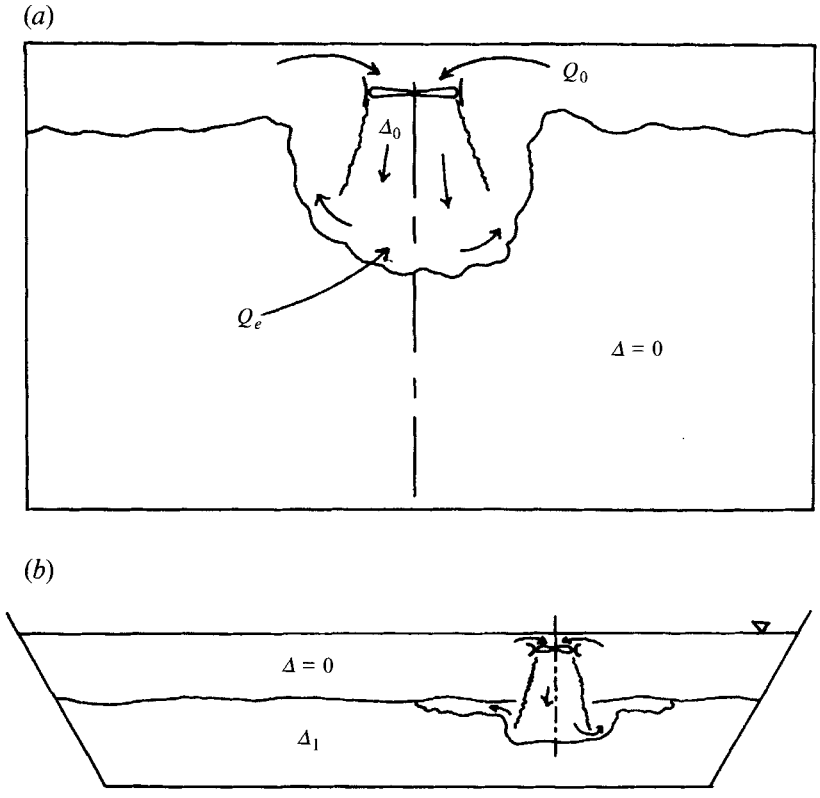

FIGURE 2. Examples of fountains in closed containers. (*a*) Fan heater at the ceiling of a cold room. (*b*) Mixing of a stratified reservoir by a propeller.

entrainment coefficient related the source properties to the penetration height. It showed that buoyancy has little effect on the upward flow over the lower 80% of the height. Turner (1966) demonstrated that the height relation was defined by dimensional analysis and found the constants from a laboratory experiment. In the tests all of the flow from the fountain was removed from the environment and this prevented the observation of how the changing environment interacted with the fountain. Seban, Behnia & Abreau (1978) studied heated air jets that were discharged downward. They concluded that the centreline temperatures and the penetration depth could be adequately predicted using a theory based only on the downward flow. Measured radial temperature profiles showed that there was substantial interaction between the core and the outer flow. Baines, Turner & Campbell (1990, hereafter referred to as BTC), studied both axisymmetric and two-dimensional fountains in an open container and demonstrated that the environmental density increased steadily with time. They found that the equation for the fountain height, derived assuming a homogeneous environment, also described the open container. It was reasoned that the weak stratification in the environment over the length of the fountain was of little consequence.

A fountain is also produced by the impingement of a jet or plume on a weak interface. The jet, or plume, penetration rises to a peak and the return flows back to the interface. This geometry was studied by Baines (1975) and Kumagai (1984), both of whom measured the total entrainment of the penetrating flow. This was shown to be a function of the local Froude number defined by the interface density difference,

the jet velocity and the width of the impinging jet. The range of Froude numbers was small in each of the previous studies and empirical equations were fitted to the measurements. Kumagai's equation when extrapolated to large Froude number predicts a maximum entrainment flux. This is counter-intuitive to the idea that entrainment is driven by the jet momentum and so should increase without limit as does the depth of penetration.

The objective of the present experimental study is the description of the density distribution produced by forced vertical motion of the environment. The imposed flow can be either in the same direction as or counter to the jet, for both of which the limiting case is a closed container. There is an exhaust at the elevation of the source of strength equal to the jet so there is no motion in the zone above the fountain. We demonstrate that in all cases the density distribution can be calculated from the conservation equations with the entrainment function.

2. Description of the flow pattern

We are examining an inherently unsteady flow although the source discharge Q_0 is steady. This commences with a variation of fountain height as the source is started. The density puff advances to an elevation where the momentum is reduced to zero. When this fluid, which is a mixture of the source fluid of density ρ_0 and the environment fluid of density ρ_i, falls back around the upward flow, the top descends to a quasi-steady level. The fluid which has been entrained from the downward flow has a density larger than ρ_i so the buoyant force exerted on the upward flow is larger. As time progresses there is gradual increase in the fountain length as the density in the environment increases. The modification of the environment is driven by the flux per unit length q_e which is entrained by the downward flow. Some of this denser fluid is transferred to the upward flow by a second entrainment process. It is more convenient to consider Q_e, which is the total entrainment between the top and an elevation z, in place of q_e because it enters the analysis directly and can be measured readily.

The height of the fountain z_m is measured from the virtual source as are all elevations z. In figure 1 the virtual source is shown to be coincident with the outlet of a pipe although in an experiment the difference between these elevations is taken into account. In general, the virtual source is a height z_s above the bottom of the container.

When the downward flow reaches the bottom, it spreads laterally and turbulence establishes a mixed layer of thickness z_e. The fluid in this layer is heavier than the environment above so mixing is inhibited. However, the entrainment flux Q_e produces an upward velocity at the top of the mixed layer and so a front of constant density moves upward. The development from this point onward depends on the volume flux imposed by the discharge Q_1 from the secondary source located above the fountain. Three cases are distinguished:

(*a*) For counterflow in the environment, $Q_1/Q_0 < 0$, the upward-directed discharge, which is Q_e, balances the downward flow from the source at a particular elevation. Thus an interface forms here and steady flow results. All of the flow Q_1 is entrained into the upper part of the fountain. Below the interface all of the entrainment comes from the mixed layer below. This provides a technique for measuring the entrainment flux. Section 5 presents results from experiments with this case and §5.1 contains a discussion of the consequences for the environment and the interaction with the fountain interaction.

(*b*) For the constant-volume container, $Q_1 = 0$, the upward-directed discharge in the environment at an elevation z is Q_e. It decreases steadily with height. As time

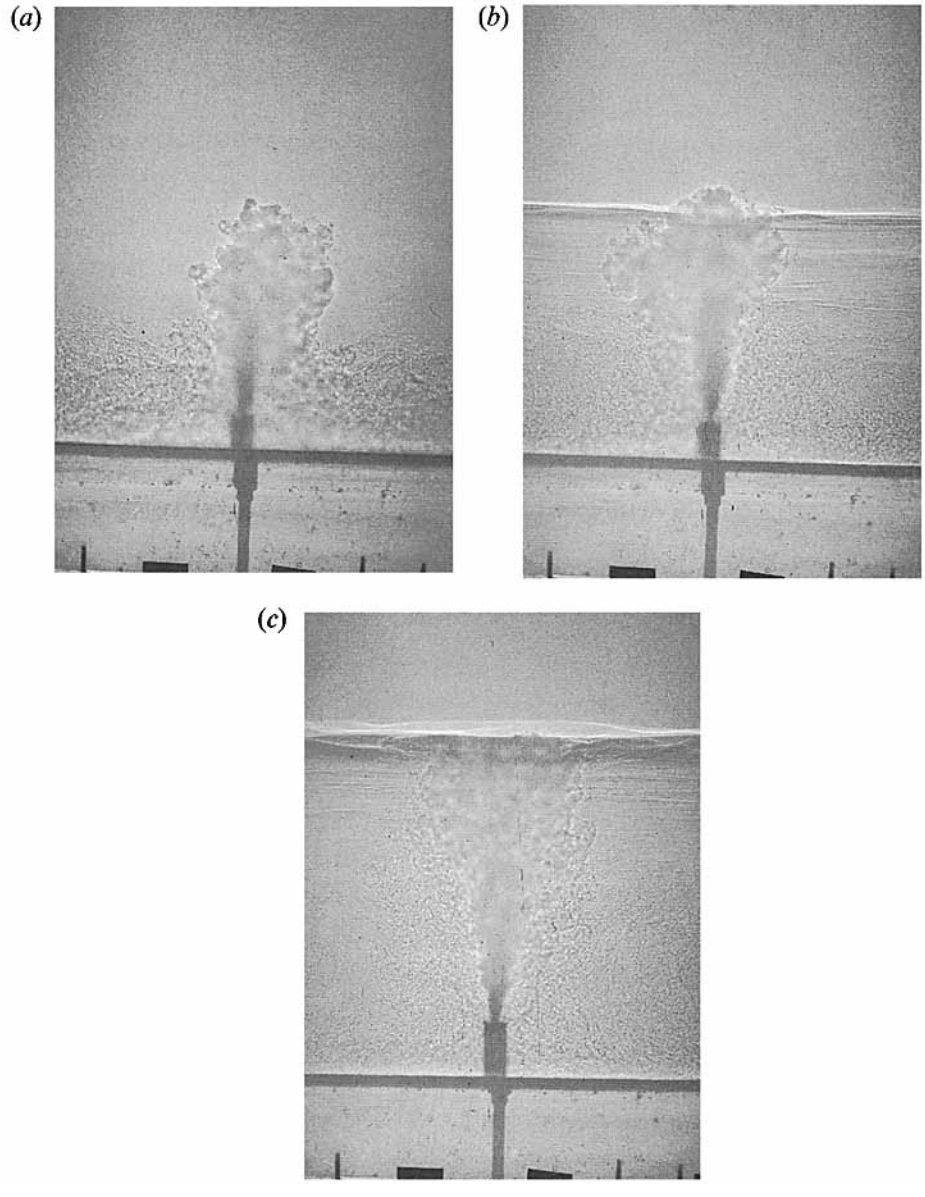

FIGURE 3. Shadowgraphs of a fountain in a container with outflow at the source elevation. Source diameter = 0.13 cm, discharge = 10.67 cm^3/s, Froude number = 54.5, $Re = 1.05 \times 10^4$. Source fluid is fresh water injected downward in a tank of salt water of density = 1.107 g cm^3. The photographs are inverted to preserve the sense of direction. The free surface is the dark line below the source. (*a*) 0.5 minutes after the start of the experiment; note the mixed layer 3 cm thick moving along the free surface. (*b*) 7 minutes after the start; the first front has moved to a level close to the top of the fountain. (*c*) 120 minutes after start; a sharp interface has developed at the top which is now flattened; the outside edge of fountain is more uniform and is of constant diameter over the height.

progresses the density of the mixed layer increases because of the continuous re-entrainment to the fountain which results in a stable density profile between $z = 0$ and $z = z_m$. As the surfaces of constant density rise, entrainment reduces the distance between them. Thus a sharp interface forms at the top where the environment velocity is close to zero. Advance at this elevation is controlled by entrainment through the end

of the fountain. The shadowgraphs of figure 3 illustrate the development of the interface at $z = z_m$. These were taken during an experiment for which fresh water was injected downward into a tank of salty water so figure 3 has been inverted to preserve the sense of this discussion. The source flow has just started in figure 3(*a*) and the turbulence in the mixed layer at the free surface is readily noted. The outer edge of the fountain is ragged and the large eddies are particularly evident. In figure 3(*b*) the first front has moved to an elevation close to z_m and the interface it formed is relatively weak. Behind the interface, the environment is striated, which shows that the mixed layer is not fully mixed, there are weak density fronts produced by the big eddies in the downward flow. The structure of the fountain is similar to that in figure 3(*a*). The third photograph was taken much later. The fountain is longer and the interface is strong, that is, the density difference is large. The end of the fountain is flat and the increase in the length indicates that there is entrainment through this end. No large eddies are seen in the downward flow part. The experiments and analysis of this case are considered in §6 for both $H > z_m$ and $H < z_m$. In the latter case the fountain impinged on the ceiling and no interface was formed.

(*c*) For the coflowing environment, $0 < Q_1/Q_0 < 1$, there is a critical value of the discharge ratio. If the rate of rise of the top is less than the velocity imposed by the upper exhaust an interface forms as in case (*b*). However, no interface forms for larger environment velocities and the density profile development is similar to that in the open container that was analysed in BTC. The analysis and results of the general case are presented in §7.

3. Dimensional considerations

For a strong source, that is one with relatively large momentum and small buoyancy, the height z_m is much larger than the radius of the source r_0 so the source is effectively a point. In this case Q_0 is not a factor and it was shown by Turner (1966) and in BTC that dimensional consistency requires that

$$\frac{z_m F_0^{\frac{1}{2}}}{M_0^{\frac{3}{4}}} = \text{constant}, \tag{1}$$

$$\frac{Q_e F_0^{\frac{1}{2}}}{M_0^{\frac{5}{4}}} = fn\left(\frac{zF_0^{\frac{1}{2}}}{M_0^{\frac{3}{4}}}\right), \tag{2}$$

where F_0 and M_0 are the buoyancy and momentum fluxes from the source divided by the density. It is convenient to introduce the Froude number of the source,

$$Fr_0 = w_0/(r_0 \Delta_0)^{\frac{1}{2}},$$

in which w_0 and r_0 are the top-hat velocity and radius, and

$$\Delta_0 = g(\rho_0 - \rho_i)/\rho_i = \text{buoyancy}.$$

Combining (1) and (2) gives

$$z_m/r_0 = C_1 Fr_0, \tag{3}$$

$$\frac{Q_e}{Q_0 Fr_0} = fn\left(\frac{z}{r_0 Fr_0}\right). \tag{4}$$

Measurements reported in BTC defined the constant C_1 in (3) as 2.46 for a vertically oriented source. If the jet is tilted by 7° from vertical, the up- and downward flows are separated and the height is increased by 17%.

In the case of a weak source z_m is of the order of r_0 and the volume flux, Q_0, of the source cannot be ignored. This is characterized by a small Froude number. These weak fountains have no distinguishable upward and downward flows. Instead, the streamlines curve and spread from the source, producing a stagnation-point type of flow. Dimensional analysis then gives

$$z_m/r_0 = fn(Fr_0), \tag{5}$$

$$\frac{Q_e}{Q_0 Fr_0} = fn\left(Fr_0, \frac{z}{r_0 Fr_0}\right). \tag{6}$$

It should be mentioned that the equations above have been derived for a homogeneous environment but are a good approximation for an environment in motion because the stratification there is weak.

4. Experimental techniques

All tests were conducted in the laboratory using fresh and salt water as the miscible fluids. Three different tanks were used and each one was constructed of glass with vertical walls so the cross-section area A was uniform. The same source was used in all tests. It was a sharp-edged orifice mounted in the end of a 1 cm diameter pipe and the jet issued at a diameter of 1.6 mm.

The tank used in the counterflowing environment was 500 mm deep with square cross-section of side 370 mm. The source for the jet of salty water was directed vertically upward from the bottom. It was metered and pumped from a tank, the density of which had been measured using a volumetric bottle. The second source which supplied Q_1 was a flow over the top edges of the tank. A double weir forming a trough was constructed around the outside of the tank at the top, and inside this trough a manifold distributed fresh water. A similar manifold was installed in the bottom of the tank to exhaust $Q_1 - Q_0$. This flow was also metered and the accuracy was $\pm 2\%$.

At the start of an experiment the fresh water flow was first established and then the source flow started. The negative jet initially rose to a height greater than the steady value of z_m and then decreased slowly as the entrainment from the downward flow part of the fountain increased. The mixed fluid from the fountain spread over the bottom of the tank and a density front moved upward until Q_1 balanced the entrainment to the top portion of the fountain. As time progressed the environment density below the interface increased and consequently the interface moved upward a small distance because the buoyant force on the negative jet had decreased. In an interval which was several times the interval required for the first front to rise to the equilibrium level, the steady state was reached. The elevation of the interface was measured using the shadowgraph technique with an accuracy of 1 mm. A series of interface elevations was then recorded by changing Q_1 by small steps. The time to reach steady state for these steps was small.

A similar technique was used for the constant-volume tests except that a jet of fresh water pointed downward below the free surface of a tank filled with salt water. The tank was 470 mm square and 600 mm deep. The same range of source Reynolds number was employed and the Froude number was varied by changing the density of salt water. For small Froude numbers the large density difference made it possible to track the fronts by a shadowgraph as seen in the photographs of figure 3. In some experiments the source height z_s varied as the free surface rose. This was accommodated in the analysis of these experiments and did not change the features of the fountain.

For a Froude number larger than 50, maintaining the same Reynolds number required the use of a density difference which was too small to give a clear shadowgraph. A technique was developed by which the density difference across a front could be fixed at a predetermined value. It was based on the principle of titration of an acid by a base. A colour-sensitive pH indicator was added to both the source and tank fluids. Phenol red was chosen because it changes distinctly from deep red to light yellow during the sharp transition in pH which occurs at the equivalence point. Hydrochloric acid was added to the salt water in the tank and sodium hydroxide to the source. The concentrations were controlled so that at a predetermined dilution of the source fluid, the entrained environment would be neutralized and the colour changed. That is, for a dilution factor n, the concentration of acid was n times that of the base. At the start of the experiment the inner flow in the fountain was red but changed before the flow reached the top of the fountain. As time progressed the environment density increased as the acid concentration decreased and the colour line progressed up to the top, down the outer flow and then into the mixed layer. A coloured region then advanced up the environment and the top edge defined the front of predetermined density. The advantage of this technique is the accurate knowledge of the density and the disadvantage is the need to repeat the experiment to define a profile.

5. Counterflow in the environment, $Q_1/Q_0 < 0$

In this case the exhaust at source level exceeds the source flow and the excess comes from the opposing flow Q_1. This is entrained by the fountain at the top and along the sides of the downward flow. At the elevation where the total entrainment $Q_e = Q_1$ an interface forms. Entrainment to the fountain at all levels comes from below. When the jet is started the first front moves to this equilibrium level and stops. As time progresses the lower region increases in density as the fluid is recirculated through the fountain until it reaches the value

$$\frac{\Delta_a}{\Delta_0} = \frac{Q_0}{Q - Q_1}, \tag{7}$$

where Δ_a is the buoyancy in the environment below the interface. This steady state provides a convenient method for determining the entrainment to the fountain since Q_1 is the entrainment flux Q_e. This technique is similar to that used to measure the entrainment to a plume by Baines (1983). There it was possible to define the entrainment flux per unit length q_e produced by a source in a uniform environment. This is not the case here. The source is in an environment of heavier fluid with the buoyancy defined by (7) and the measured entrained flux comes from lighter fluid. Nevertheless the measured Q_e must follow the form of (4) although it is not the one that applies to a uniform-density environment.

Figure 4 is a plot of the measurements using (4). There is very little scatter and the points approach a straight line with slope $= -0.25$ for $z \to 0$. At small z the density difference is small so in this region this line describes the uniform-density case. This line also passes through the point for z_m defined by (3) at $Q_e = 0$ and so it should describe the uniform-density case for large z. It is reasonable to conclude that in a uniform environment the entrainment per unit length is

$$q_e = B Q_0 / r_0, \tag{8}$$

where B is the entrainment coefficient, which is 0.25 in this case.

With this step density profile, the momentum of the inner or upward flow is larger at the interface than it would be were all of the environment composed of the upper

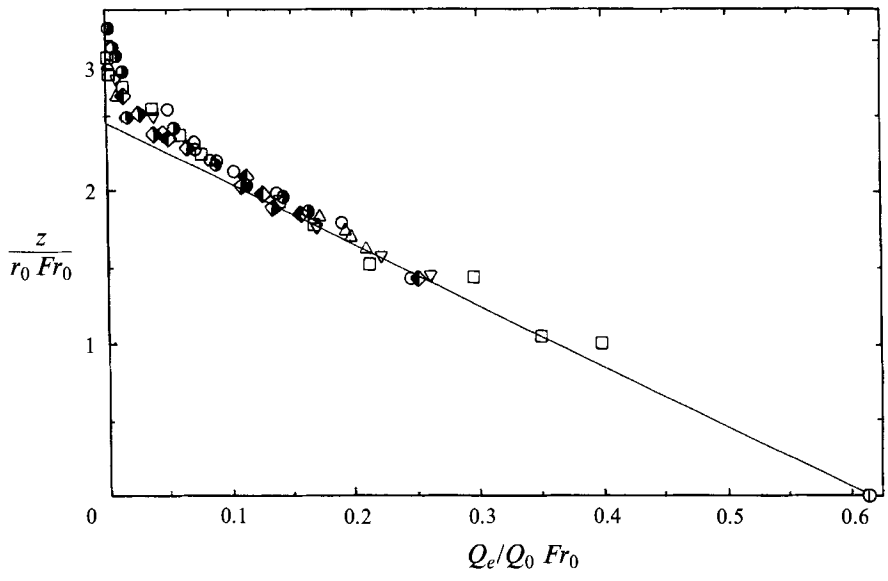

FIGURE 4. Dimensionless entrainment flux into the top part of a fountain as measured from the flow entering the fountain above an established interface. Solid line is $Q_e/Q_0 Fr_0 = 0.611 - 0.25\, z/r_0 Fr_0$. ◆, $Fr = 31.6$; ◈, $Fr = 35.4$; □, $Fr = 42.0$; ▽, $Fr = 56.3$; ○, $Fr = 57.8$; ⊕, $Fr = 70.6$; △, $Fr = 79.6$; ◑, $Fr = 102.7$.

fluid. The jet flows through the heavier fluid below the interface with a smaller buoyancy force and so it reaches the interface with more momentum. This produces larger entrainment after it penetrates the interface and so the measured entrainment deviates progressively from the line on figure 4 as the interface approaches z_m.

Impingement of a jet or plume on an interface is a similar flow. This was studied by Baines (1975) and Kumagai (1984) who measured the flux entrained by a vertical jet or plume. The mixture of fluid which flowed back to the interface had a density that was intermediate between that of the undisturbed fluids above or below the interface. Thus the outflow accumulated in a third layer between the two. The fountain in a moving environment does not produce a mixed layer but the flows are otherwise identical. In this case all of the fluid in the environment above the interface comes from the upper source. Below the interface the fluid recirculates through the lower part of the fountain. The density at a point does not vary with time so from the conservation of buoyancy the density gradient must be zero. Thus the density of the outer or downward flow part as it crosses the interface must be the value given by (7). This flows as an annular jet in the lower region and its effect on the upward flow is much less than the accelerating annular downward flow in a uniform environment. The upward flow has a constant buoyancy flux and the velocity and density difference profiles are probably close to Gaussian. Thus the entrainment above the interface should be comparable to an impinging density for which it was deduced that Q_e is a function only of the local properties of the jet or plume at the elevation of the interface. Dimensional consistency requires that

$$\frac{Q_e}{\pi w_1 b_1^2} = fn\left(\frac{w_1}{(b_1 \Delta_{12})^{\frac{1}{2}}}\right) = fn(Fr_G), \tag{9}$$

where w_1 is the centreline velocity of jet at elevation of the interface, b_1 is the radius of the jet where the velocity is w_1/e, and Δ_{12} is the difference in density between the jet

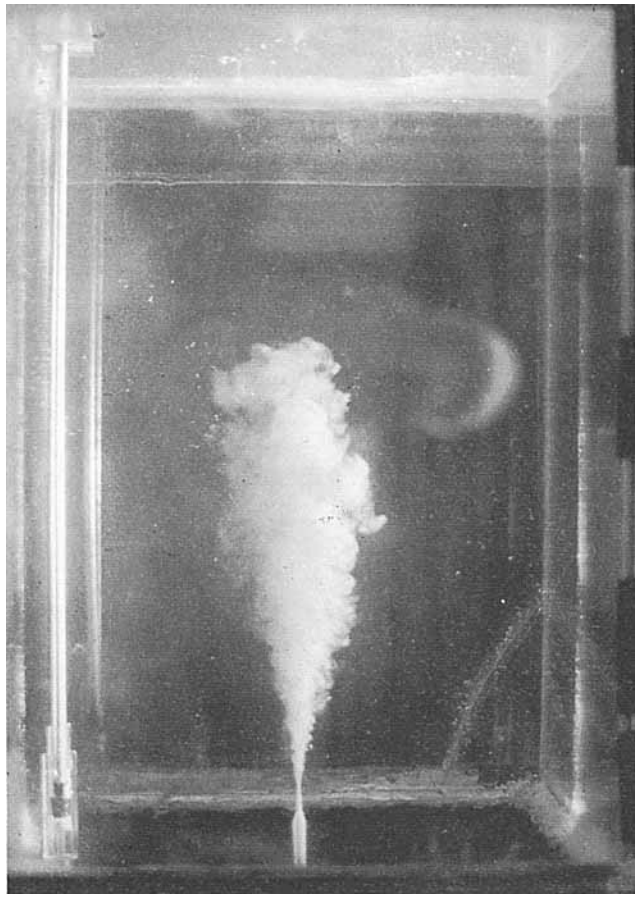

FIGURE 5. Photograph of the upflow region of a fountain. Dye was injected in the source and the photograph taken as it reached the top. Note the linear spread from the source to an elevation about one diameter from the top.

and the fluid above the interface. Fr_G is the local Froude number; the subscript G denotes Gaussian profiles. This is equal to a Froude number based on top-hat profiles multiplied by $2^{\frac{3}{4}}$.

The data on figure 4 can be cast in these variables once b_1 and w_1 are determined. This has been accomplished using the integral analysis used for a positive jet or a plume. There are two approximations which could be adopted. Morton (1959) assumed a constant entrainment coefficient and found that the properties are, within a few percent, identical to those of a jet from the source to $0.8z_m$. Above this level the negative jet spreads faster. At $z = z_m$ the width is infinite, the velocity is zero and the volume flux finite. Crapper & Baines (1978) assumed a linear spread and found that the volume flux increased to a maximum at $0.8z_m$ and decreased to zero at the top. Both approximations probably provide a reasonable description for $z < 0.8z_m$ but not above this level because the radial velocity is large. The photograph of figure 5 shows the upward flow region in a fountain in a uniform environment. Dye was injected into an established flow and the photograph taken as the first particles reached the top. The linear spread for $z < 0.8z_m$ is clearly seen. The conical top is the result of the eddies in the centre moving faster than those on the edges. This linear spread has been adopted for the definition of the local properties of the upward flow. For Gaussian distributions

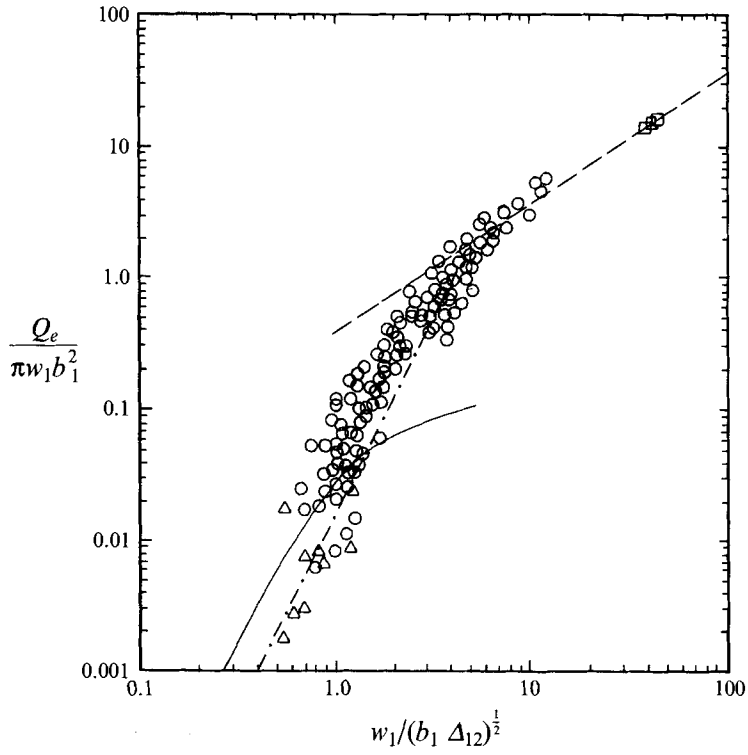

FIGURE 6. Ratio of entrainment flux to inner flow flux as a function of the Froude number of the impinging flow: △, measured by the established interface; □, measured by moving the source to maintain the interface at the source elevation; ○, inferred from the advance of the fountain seen in figure 3. Long-dash line is the line on figure 4, $Q_e/Q = 0.363\,Fr_i$. Dash-dot line is the mean of data from Baines (1975), $Q_e/Q = 0.015\,Fr_i^3$. Solid line is the mean of data from Kumagai (1984), $Q_e/Q = 1/((42.25/Fr_i^3)+(23.15/Fr_i)+5.65)$.

of both velocity and buoyancy, the conservation equation for momentum divided by the density is

$$\frac{\mathrm{d}}{\mathrm{d}z}(\tfrac{1}{2}\pi w^2 b^2) = -\pi\lambda^2 \Delta b^2, \tag{10}$$

where λ is the ratio of radii of buoyancy and velocity profiles. Inserting the linear spread

$$b = 2\alpha z, \tag{11}$$

where α is the entrainment coefficient for a jet. Integrating (10) gives the velocity

$$w^3 = \frac{1}{z^3}\left[\left(\frac{M_0}{2\pi\alpha^2}\right)^{\frac{3}{2}} - \frac{3(1+\lambda^2)F_0}{8\pi\alpha^2}\left(z^2 - \frac{b_0}{4\alpha^2}\right)\right], \tag{12}$$

where b_0 is the effective radius of the profile at the source. The first term on the right-hand side is the momentum flux at the source and the second term is the momentum reduction by the buoyant force.

All the measurements of Q_e are plotted in the variables of (9) on figure 6. These cover the full length of fountains with source Froude number Fr_0 between 25 and 100. The mean lines of the measurements reported by Baines (1975) and Kumagai (1984) are plotted on the same figure. The range of Froude number is larger than either of the previous studies and can be separated into two regions. The linear relationship for

$Fr_G > 5$ is the result of a constant entrainment coefficient and corresponds to the point at $z = 0$ on figure 4. The limiting value of $Fr_0 = 5 \times 2^{\frac{3}{4}} = 8.4$ defines the minimum for a strong source for which entrainment is independent of the volume flux. This linear relation is not consistent with the equation proposed by Kumagai (1984) which approaches a constant value at large Froude number. This would require that q_e be inversely proportional to Fr. That is, entrainment would decrease as the momentum of the negative jet increases. This is not consistent with the argument that entrainment is driven by the momentum of the shear flow.

For $Fr < 5$ entrainment is smaller than the linear relation and the mean line is

$$\frac{Q_e}{\pi w_1 b_1^2} = 0.08 Fr_G^3. \tag{13}$$

The same cubic relation was seen in the data of Baines (1975) and Kumagai (1984) but the constant was larger.

The reason for the smaller entrainment for $Fr_G < 5$ lies in the flow field in the impingement zone. The fountain penetration z_m is of the order of b_0 or r_0. Thus the streamline curvature starts at the source and there is rapid radial deflection. The vertical inertia of the fluid particles is less and this reduces the entrainment. From the dimensional analysis discussed above, the volume flux would have to be included and the result is (6) with z set to zero. This is not necessarily a linear relation.

5.1. *Consequences of constant entrainment flux*

These measurements of q_e indicate that it is constant in a uniform environment. This is assumed to be a good approximation for the weak stratification between the source and z_m. This leads to a simple derivation for the motion of the density fronts generated by the mixed layer at the bottom. Because of the stable stratification and the small velocity, the pressure distribution is hydrostatic. The entrainment to the fountain is similar to a line sink and it is drawn from the elevation where it enters the fountain. Thus the flow is one-dimensional. In addition the Péclet number is large enough for diffusion to be neglected. A fluid particle leaves the mixed layer with the instantaneous density of that in the layer and is effectively a density front. At a later time a second particle with a larger density leaves and the distance between the two is δz_0. As these move along the fountain the continuity equation is

$$A \frac{\mathrm{d}\delta z}{\mathrm{d}t} = q_e \delta z. \tag{14}$$

Combining this with (7) and integrating gives

$$\delta z = \delta z_0 \mathrm{e}^{-Bt'}, \tag{15}$$

where $t' = Q_0 t / A r_0$ is the dimensionless time. The spacing reduces exponentially with time.

The transit time for a front to move from the mixed layer to the top of the fountain is found from the environment velocity

$$W = \frac{\mathrm{d}z}{\mathrm{d}t} = \frac{Q_1}{A} + \frac{BQ_0}{Ar_0}(z_m - z), \tag{16}$$

which is a function of time because the fountain lengthens as the environment becomes more dense. An approximate solution was obtained in BTC for the case of a weak environment buoyancy gradient which gave a linear growth rate for the fountain

$$z'_m = z'_{mi}(1 + \tfrac{1}{2} z_r t'), \tag{17}$$

where lengths have been made dimensionless by division by r_0, and z_r is the ratio $z_m/(z_m+z_s)$. Note that z_s is the elevation of the source above the bottom of the tank. Integration of (16) now gives

$$z' = (z'_e - z'_s)\,\mathrm{e}^{-Bt'} + \left[z'_{mi} + \frac{1}{B}\left(\frac{Q_1}{Q_0} - \frac{z_r}{2}\right)\right](1-\mathrm{e}^{-Bt'}) + \tfrac{1}{2}z_r\,t' \tag{18}$$

and the transit time t^* for the front to reach the elevation z_m is

$$t^* = \frac{1}{B}\ln\left[\frac{B(z'_{mi}+z'_s+z'_e)+Q_1/Q_0-\frac{1}{2}z_r}{Q_1/Q_0-\frac{1}{2}z_r}\right]. \tag{19}$$

It is evident that t^* increases as Q_1/Q_0 decreases from unity, which is the value for an open container, and for $Q_1/Q_0 \geqslant \frac{1}{2}z_r$, t^* is infinite.

Since the density or any scalar property remains constant as it moves upward, the buoyancy gradient in the environment, Δ_a, is given directly by (14) written in Lagrangian variables

$$\frac{\mathrm{d}\Delta_a}{\mathrm{d}z} = \frac{1}{W}\frac{\mathrm{d}\Delta_e}{\mathrm{d}t}\mathrm{e}^{Bt'}, \tag{20}$$

where W and Δ_e, which is the buoyancy in the mixed layer, are evaluated at the instant when the front leaves the mixed layer. For large t^* the buoyancy gradient at the top of the fountain is very large and in the limit of $t^* \to \infty$ there would be a step. Molecular diffusion cannot be neglected in that case and the step is replaced by an error function profile.

6. Constant-volume container, $Q_1/Q_0 = 0$

This case is analogous to a fountain produced by a heat source and is produced by exhausting the source flux Q_0 at the source level.

6.1. *Deep tank*, $H > z_m$

These experiments were conducted in a deeper tank where the fountain could lengthen throughout the run. Figure 7 presents the measured location of the first front which was observed by introducing dye into the starting jet. This is a typical case of moderate Froude number. The points follow a smooth curve which rises rapidly until the front approaches z_m. It then develops into an interface which strengthens as time progresses. The top flattens and merges into the interface. The points agree well with an approximate solution of the conservation equations of volume and buoyancy. These equations are derived for the general case of $Q_1 \geqslant 0$. First, the conservation of volume for the zone above the interface gives

$$\frac{\mathrm{d}z}{\mathrm{d}t} = \frac{1}{A}(Q_e+Q_1), \tag{21}$$

where the entrained flux Q_e is defined by the two relations on figure 6. To evaluate Q_e requires the evaluation of w_1 and b_1, which are the velocity and radius in the upward flow, as well as the buoyancy difference between the jet and the fluid above the interface. The jets properties are calculated by (11) and (12) for the source fluxes, where z is the interface elevation. The buoyancy difference is the buoyancy in the jet plus the buoyancy in the environment below the interface

$$\Delta_{12} = F_0\frac{\Delta_0-\Delta_a}{\Delta_0}\frac{1+\lambda^2}{\lambda^2 Q} + \bar{\Delta}_a, \tag{22}$$

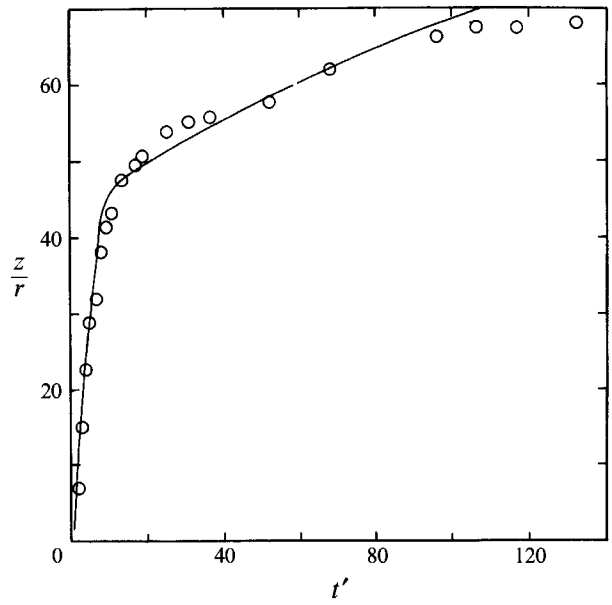

FIGURE 7. Dimensionless plot of the advance of the first front in a closed container. This forms the strong interface at the end of the fountain seen in figure 3. Points are the measured location of the first front which develops into an interface. Solid line is (18). $Fr_0 = 20.7$.

where Δ_a is measured at the lower side of the interface, and the mean buoyancy $\bar{\Delta}_a$ in this zone below the interface is used as an approximation to the local buoyancy. It is calculated by integrating the equation of conservation of buoyancy below the interface

$$\frac{\mathrm{d}}{\mathrm{d}t}[\bar{\Delta}_a(z+z_s)] = \frac{1}{A}[Q_0(\Delta_0-\Delta_e)+Q_1\Delta_e]. \tag{23}$$

In the initial interval as the first front moves quickly up the fountain and $Fr_G > 5$ the entrainment q_e is constant so, as noted above, (13) leads to (18) for the interface elevation. The mean density is consequently

$$\bar{\Delta}_a = \frac{\Delta_0}{A(z+z_s)}Q_0 t. \tag{24}$$

It is thus possible to calculate the time when $Fr_G = 5$ and use the results for z and Δ_a as the starting conditions for a numerical solution of (21) and (23) with Q_e defined by (13).

Figure 8 is a plot of the solution for the variation of mean environment density with time. The points are samples taken 1 cm from the free surface where $z = z_s$ and hence would be expected to be of slightly higher density than the mean. The scatter, which is primarily due to inaccuracy in density determination by the volumetric bottle, does fall around the calculated line so this approximate solution gives a reasonable description of the development of the interface.

The fronts defined by the titration technique produced similar curves for z variation with time. Figure 9 is a plot of the front with dilution $\Delta_0/\Delta_a = 56$ in a fountain with $Fr_0 = 55.5$. The solid curve is a numerical solution for the front based on the constant entrainment coefficient and the dashed curve is the solution for the top of the fountain. This solution, which is an approximation to the full solution described in the paragraphs above, accounted for the buoyancy distribution in the environment using

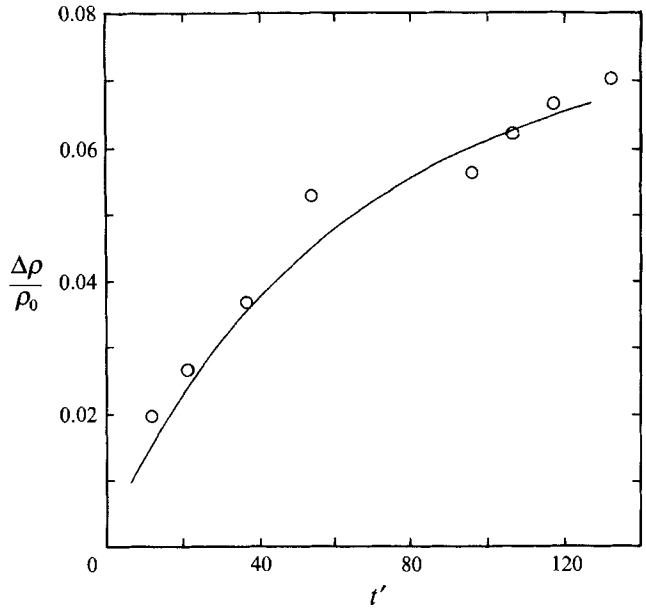

FIGURE 8. Mean buoyancy below the interface in the environment of a closed container for the experiment in figure 7. Points are the density of samples drawn from an elevation 1 cm below the free surface. Solid line is an approximate numerical solution for a strong interface.

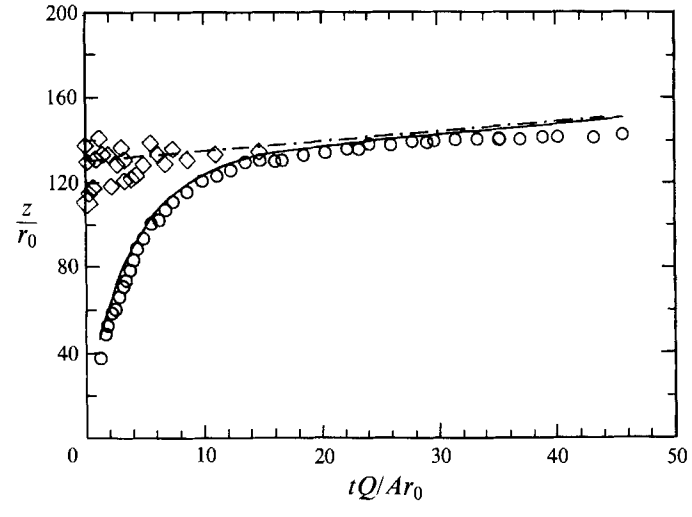

FIGURE 9. Advance of a front of defined density in a closed container. Froude number = 55.5. The indicator in the source fluid changed colour at a density difference = $0.0175\Delta\rho$; ○, location of the front; ◇, top of the fountain. Solid line is the numerical solution for the front location, and the dashed line is the solution for the top. The numerical solution is based on a weak interface so the slope of the lines is $\frac{1}{2}z_r$ after coincidence. The front and top advance more slowly at large time because of reduced entrainment through the top of the fountain.

(18) to track the density originating in the mixed layer and is an extension to the solution developed in BTC. The agreement with the observed front is good up to a dimensionless time of 30. For larger time the front advances more slowly because Q_e here is given by (14) and is smaller than the value given by the linear variation with Fr.

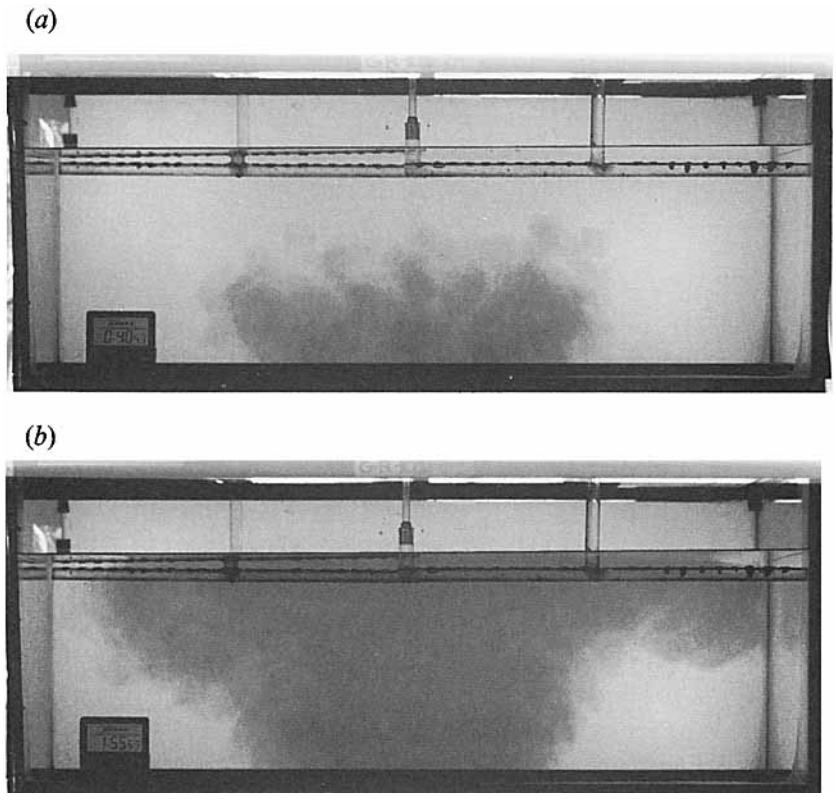

FIGURE 10. Photographs of a fountain in a shallow tank. $Fr_0 = 141.6$; (*a*) $t' = 0.41$, (*b*) $t' = 1.18$.

6.2. *Shallow tank*, $z_m > H$

In this case the starting phase was an appreciable proportion of the time needed for the front to transverse the depth H. The ring vortex or puff at the end of the starting fountain played an important role in the mixing of fluid in the container. This puff expanded as the fountain started and impinged on the container top surface. It then responded to the image vorticity and expanded rapidly to occupy a large volume. The photograph of figure 10(*a*) shows an outside diameter about 3 times the diameter of the jet upon impact. The expansion in diameter increased as z_m/H was increased. This is to be expected since the advance velocity of the puff decreased with height because of negative buoyancy. The upward motion stopped at the ceiling and the vortex fell back to the source elevation. There it spread laterally to the sidewalls and formed the mixed layer. Figure 10(*b*) shows the vortex approaching the sidewalls. It also shows that the established downward flow in the fountain was much wider than the upward flowing jet. The diameter of this downward flow also increased with z_m/H and this may explain why the calculated entrainment coefficient was larger than the value 0.25 measured in BTC. The values from the experiments were determined by comparing the measured location of the front with the numerical solution of (17). The coefficient B was varied with time in the solution. The results closely followed the empirical relation

$$B = 0.25(1+2\,\mathrm{e}^{-t'})(z_m/H)^2. \tag{25}$$

The decreasing exponential term was introduced to describe the initial puff because the strength of the puff velocities were seen to decay rapidly with time. The effect of the

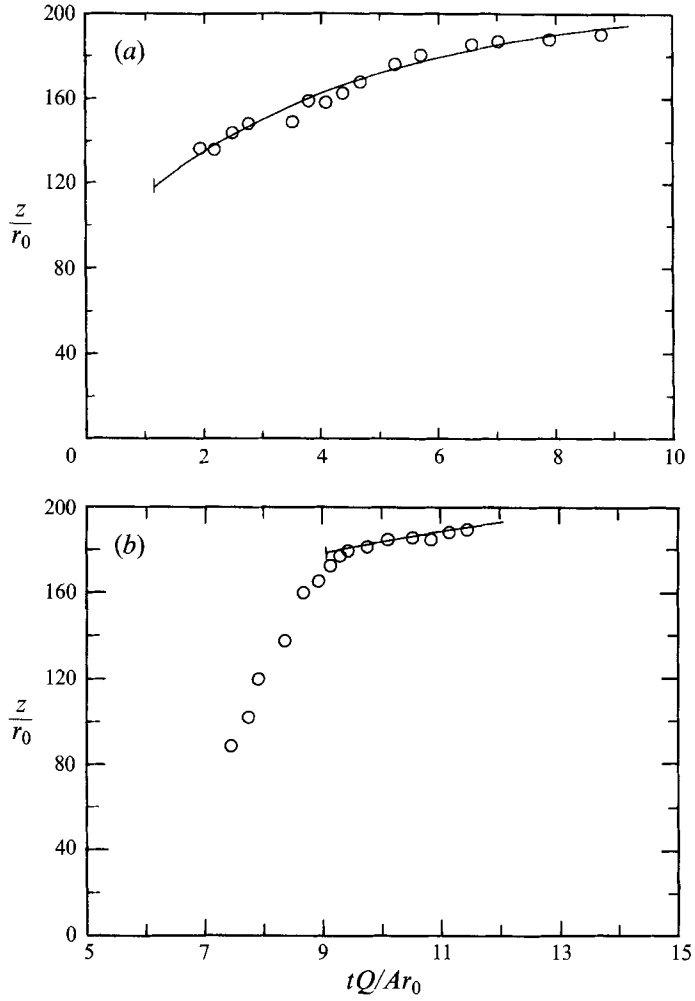

FIGURE 11. Position of a front of defined density in the environment of a shallow tank. (*a*) $Fr_0 = 96.4$, density difference $= 0.0077\,\Delta\rho_0$. The fountain impinges on the wall at $z/r_0 = 211.5$ and a thick mixed layer forms on the opposite wall. Solid line is numerical solution. (*b*) $Fr_0 = 136.6$, density difference $= 0.043\,\Delta\rho_0$. Solid line is the numerical solution which starts at $t' = 9.1$ when the numerical mean density reaches the preset value of the experiment.

increased diameter of the steady fountain which followed the puff was described by the square term in (25). Examples of the agreement between the numerical solution and the measured front location are given on figures 11 (*a*) and 11 (*b*). The short vertical line on the left end of the curve indicates the time when the front colour change should make it visible. However the front could be identified before this time because the fluid density is not uniform. Mixing is not complete, especially near the sides of the tank. The excellent agreement seen on these plots indicates the accuracy of (25) in defining the entrainment coefficient.

An increase of the source Froude number increased the strength of the initial puff and the size of the zone it mixed after impact. When this zone approached the size of the tank the effect of the jet in the mixing process was small. Fronts are not formed and mixing is not influenced by buoyancy. In these experiments with $H/r_0 = 212$, this limit was observed to be $Fr_0 = 200$ which is a height ratio $z_m/H = 2.33$. Two photographs

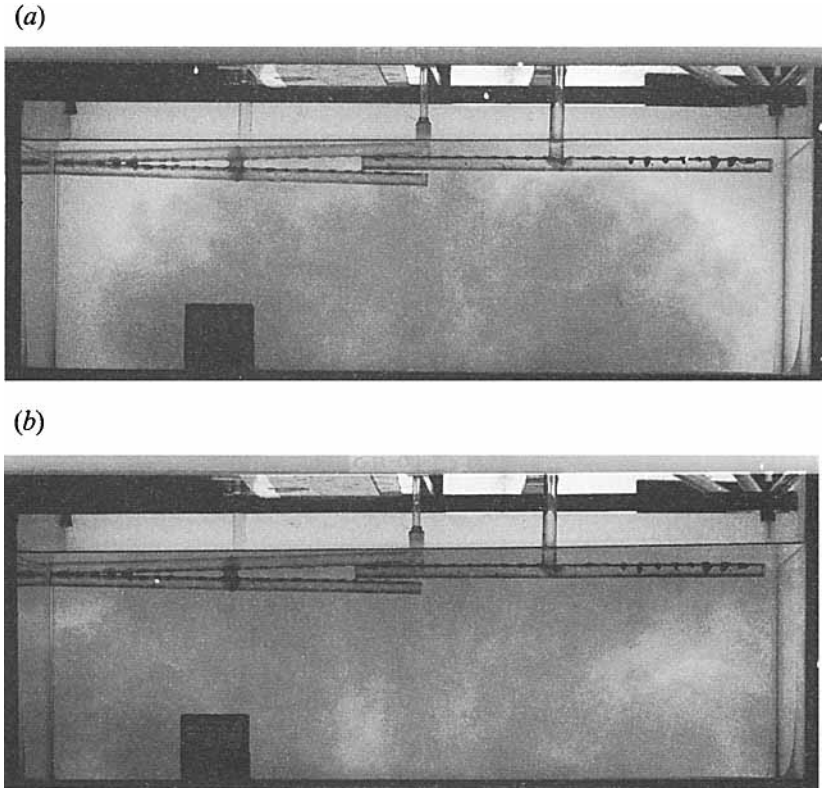

FIGURE 12. Photographs of a fountain with large momentum in a shallow tank. The ring vortex which is formed at the top of the starting phase expands rapidly and occupies the whole depth. $Fr_0 = 487.8$; (*a*) $t' = 1.01$, (*b*) $t' = 1.68$.

of this case are presented in figure 12. The first one shows the puff which after impact has expanded to a size of about $\frac{1}{2}H$. The second photograph taken 15 s later shows the edges to be at the tank walls and there are small regions which have not been diluted to the preset value. This condition can be used to define an approximate mixing time t_1 for the mean dilution to reach the defined value. Several dilutions were tested at each of four source Froude numbers and the results agreed within a few percent of the equation for perfect mixing

$$t_1 = \frac{HA}{Q_0} \ln\left(\frac{A_0}{A}\right), \tag{26}$$

that is, the consequence of the concentration being uniform at all times.

7. Coflow in the environment, $1 > Q_1/Q_0 > 0$

The development of this fountain has been deduced in §3 by considering the relative motion of the top and the environment. This leads to (19) from which it is seen that the interface should form at the top if $Q_1/Q_0 < \frac{1}{2}z_r$. For Q_1/Q_0 larger than this limit the environment moves faster than the top, which is exactly the case in the analysis developed in BTC. An increase in Q_1 is accompanied by a decrease in the interval required for a front to move to the top and a decrease in the density gradient in the environment. Thus the gradient passed on to the region above the fountain decreases.

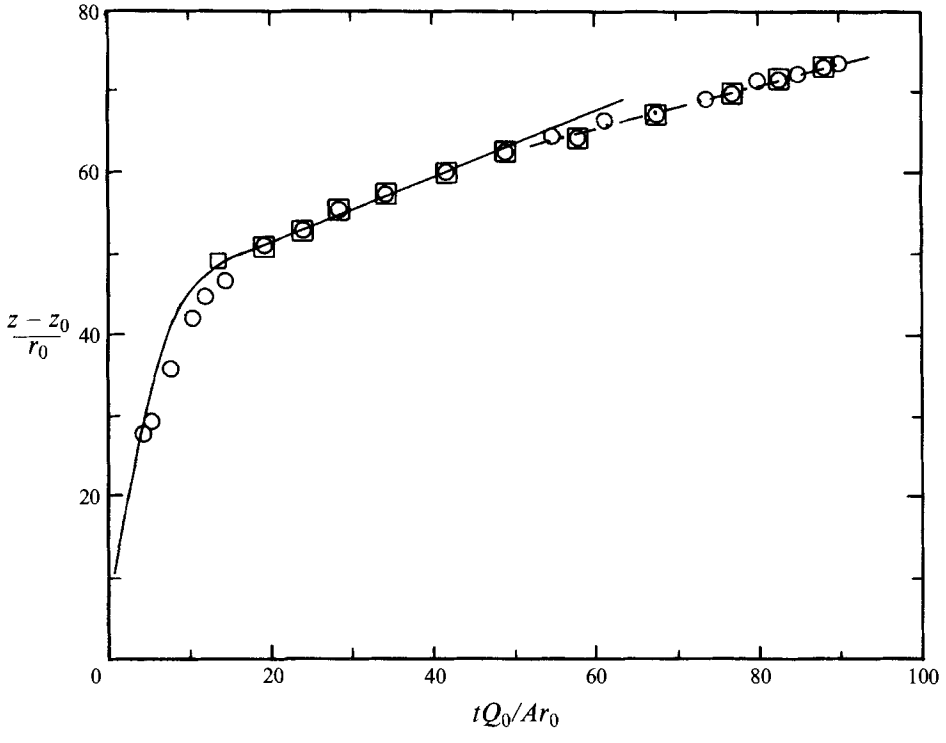

FIGURE 13. Advance of the first front for $Q_1 = 0.25\,Q_0$. The top and front are coincident after $t' = 20$. The solid line which describes the position up to $t' = 45$ is an analytical solution based on the assumption of a weak interface. Dashed line has the slope of the particle velocity in the environment. ○, First front position; □, top location.

For $Q_1/Q_0 < \frac{1}{2}z_r$ an interface should form but the density difference across it decreases as the limit is approached. A series of experiments was conducted in the 47 cm square tank to verify the existence of the two cases and the accuracy of the numerical solutions for the density profiles.

Data from an experiment in which an interface forms are plotted on figures 13 and 14. Here $Q_1/Q_0 = 0.25$ and $\frac{1}{2}z_r \approx 0.33$ so the growth of the fountain is faster than the particle velocity. The progress of the first front can be seen in figure 13. The circles show the measured front position and the squares show the top elevation. The two are coincident after $t' = 20$ and for a short while the front and top advance at the rate in an open container. The strength of the interface increases steadily because there is no flow across it. It would be expected from the numerical solution described in §3 that the rate of advance would decrease and approach the particle velocity Q_1/A when the entrainment Q_e is very small. The measurements show the change in the rate, but it is sudden. At $t' = 50$ there is a break in the curve. This shows that there is a change in the entrainment or the structure at the top which is not described by the analogy to jet impingement on an interface. The density points plotted on figure 14 shows the sharp interface with spreading due to molecular diffusion. The line is the numerical solution derived in BTC and this is in good agreement with the measurements. It should be noted that this solution does not include the variation of entrainment with Froude number but it is based on a constant entrainment coefficient. The duration of the experiment was too short to show the effect of the strong interface on the density profile.

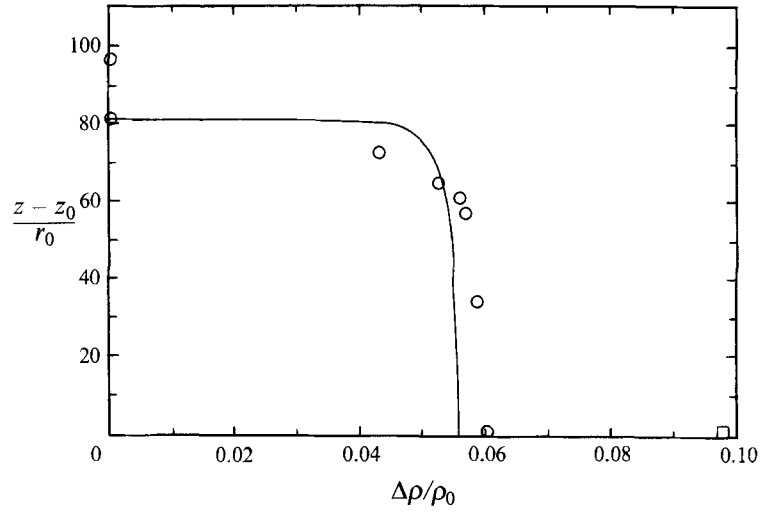

FIGURE 14. Buoyancy distribution in the environment for $Q_1 = 0.25\,Q_0$. Points were measured after $t' = 89.6$. Solid line is calculated from a numerical simulation in which diffusion was neglected. ○, Density distribution; □, source density.

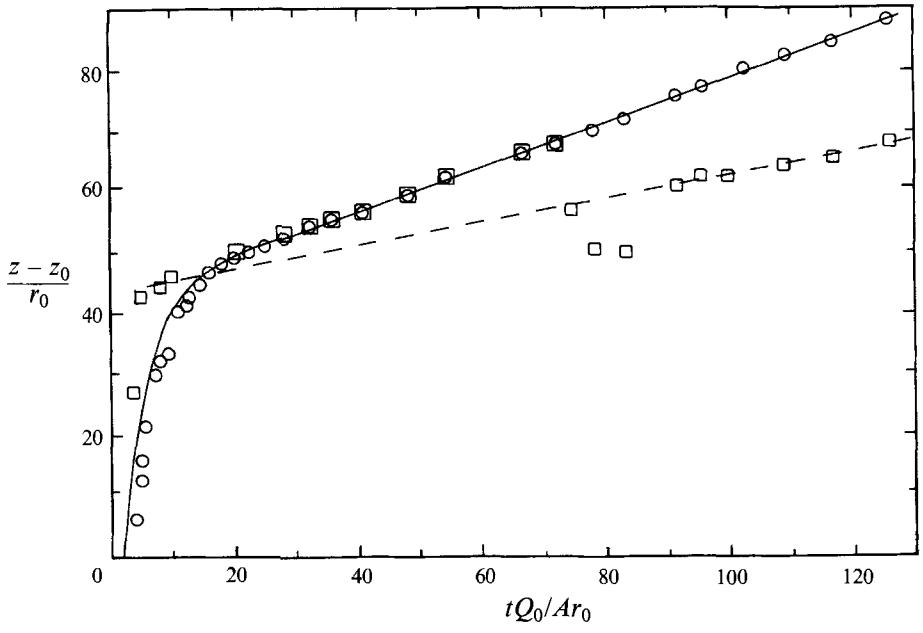

FIGURE 15. Position of the first front and the top of the fountain for $Q_1 = 0.375\,Q_0$. Solid line is the analytical solution based on a weak interface. Dashed line is the top advancing with a velocity of $\frac{1}{2}z_r$. Note that the top follows the front from the time of coincidence to $t' = 70$ when it drops to the dashed line. ○, Measured front position; □, measured top location.

In the next case examined $Q_1/Q_0 > \frac{1}{2}z_r$ so the first front should pass the top of the fountain as in an open container. Figure 15 presents the measurements of the position of the first front and the top, along with the analytical solution as a solid line. In the interval from $t' = 0$ to $t' = t^* = 20.7$ the front rises to the top and the measurements agree well with (17). The top advances at the speed $\frac{1}{2}z_r$ within a band of scatter. For

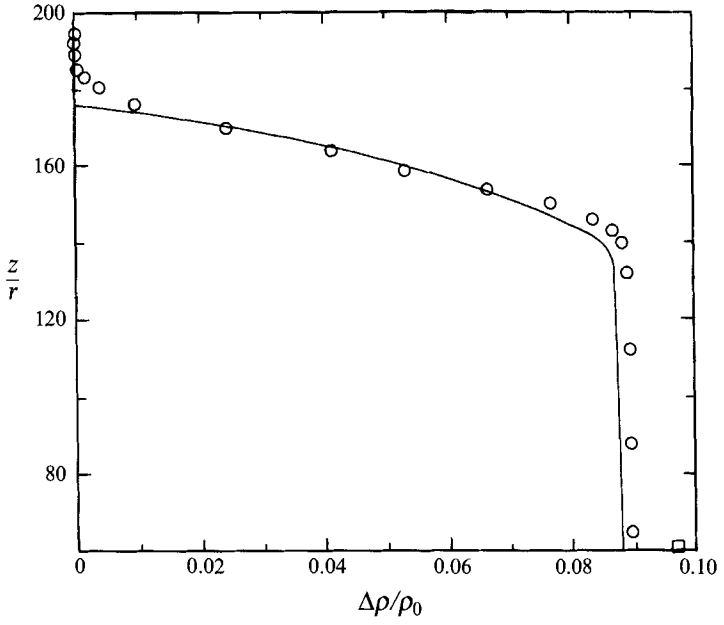

FIGURE 16. Buoyancy distribution at $t' = 358$ for $Q_1 = 0.375\,Q_0$. Solid line is a numerical simulation which assumes the top follows the dashed line on figure 15. ○, Measured density distribution; □, measured source density.

$t' > t^*$ the front advances with the dimensionless particle velocity, which is Q_1/Q_0 as in an open container. However, the motion of the top of the fountain is not as would be expected from the previous experience with fountains in an open chamber. In the interval from t^* to $t' = 75$ it does not oscillate and moves with the first front. Then at $t' = 75$ it drops suddenly and the oscillations are again observed. From this time on it advances at the rate $\frac{1}{2}z_r$ as was developed in BTC. The reason for this linking of the top to the first front must be a change in the structure of the fountain produced by the interaction of the motion of the top with the weak interface which is the first front. The photographs in figure 3 show a different fountain outline for cases of impingement and weak interface. Measurements of the density profile did not, however, show an effect of this linkage. Figure 16, which is the plot of the measurements taken at the end of the experiment and a numerical solution of the conservation equation, demonstrates this conclusion.

In the third case the first front passed the top with a larger relative velocity and the linking of the top to the passing front was noted again. Figure 17 is a plot of the front and top along with the same solution. The top rose with the front from $t' = t^* = 18.1$ to $t' = 26$, at which point it dropped back to the rate $\frac{1}{2}z_r$. A second interface could be seen at $t' = 42$ and this rose to the top and then continued at the particle velocity. The time interval between $t' = 26$ and reaching the top is equal to t^* calculated for the conditions at $t' = 26$. This shows that the second interface which could be seen clearly on the shadowgraph is the steepening of the density profile caused by the top departing from the first front. It is not discernible at low elevations but the steepening produced by entrainment makes it visible. An additional five interfaces were observed during the remainder of the experiment. Most were produced by the top following the weak interfaces previously created. The density profile measured at $t' = 356.5$ and plotted on figure 18 show that the interface has bulges on an otherwise smooth curve. The solid

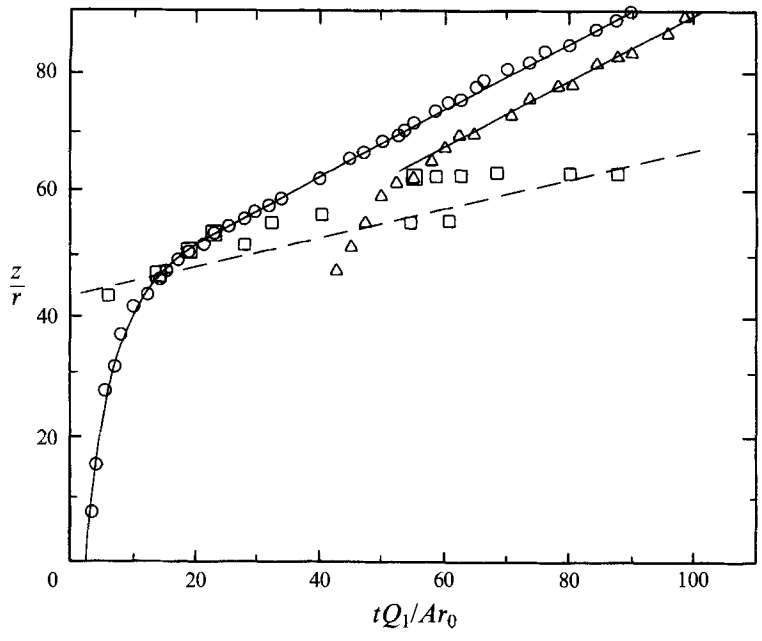

FIGURE 17. Position of fronts defined by the white lines on a shadowgraph for $Q_1 = 0.583\,Q_0$. Solid line is an analytical solution based on a weak interface. Dashed line is the top advancing with velocity $\frac{1}{2}z_r$. Note that the top follows the first front from t^* and $t' = 25$ and the second front from $t' = 47$ to $t' = 57$. ○, First front position; △, second front position; □, top location.

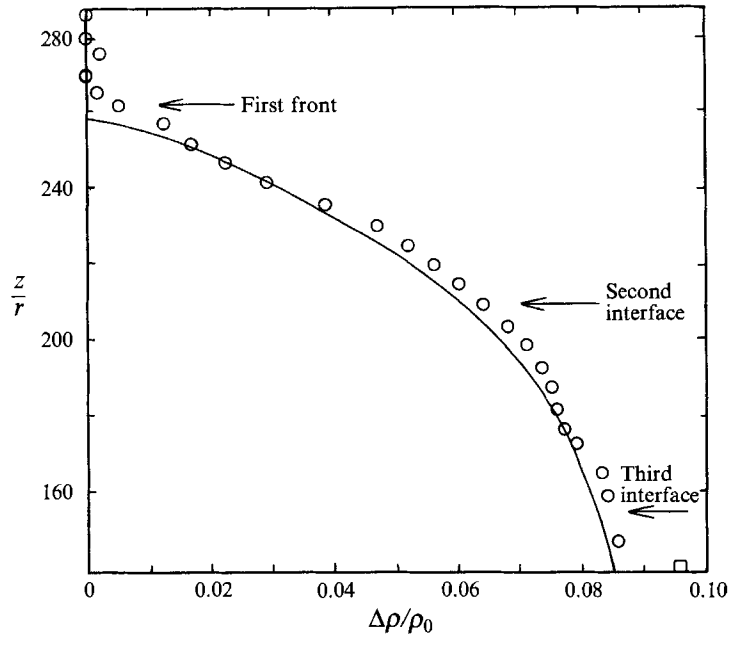

FIGURE 18. Density distribution at $t' = 356.5$ for $Q_1 = 0.583\,Q_0$. Solid line is a numerical simulation which assumes the top follows the dashed line on figure 17. The bumps on the measured curve act as lenses and so produce the white lines on the shadowgraph. ○, Density distribution; □, source density.

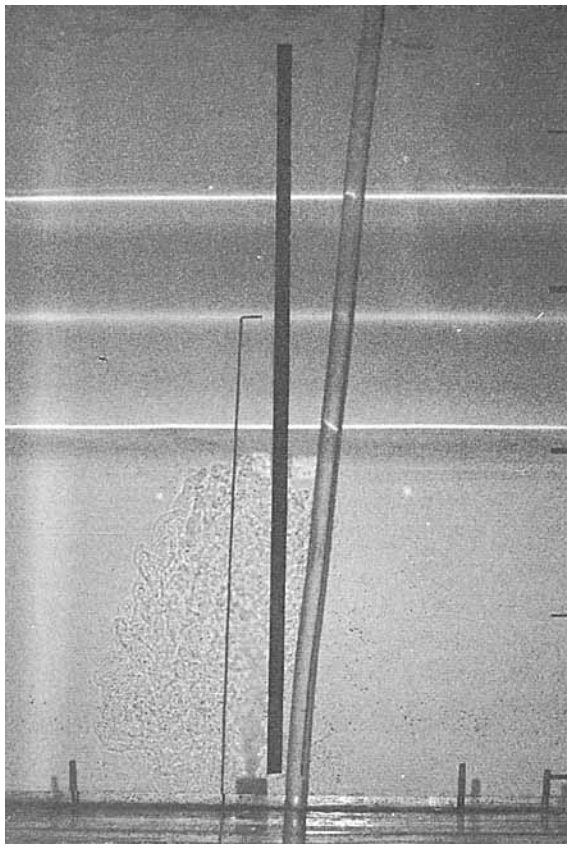

FIGURE 19. Shadowgraph of the experiment documented in figures 17 and 18 at $t' = 238.6$. Three white lines are evident. Fluid above the highest line was at the top of the fountain at $t' = 0$.

line which is a numerical solution of the conservation equations follows the trend of the measurements and emphasizes the bulges. When the top drops suddenly, the density of the mixed layer increases rapidly because entrainment is coming from a denser zone. This accelerated increase in density when steepened appears as flat region in the density profile at t^* later. Several of these bulges can be seen on figure 18. Each one functioned like a lens in the shadowgraph producing a pair of light and dark lines as seen on the photograph of figure 19. The highest interface is the first front and the two sharp ones below it coincide with the two bulges seen on figure 18. There is a strong deflection of the optical path so the observed positions do not fit with the bulges in the profile. The other four interfaces observed during the experiment have been weakened by diffusion so are not seen clearly.

The reason for the unexpected growth of the fountain must lie in the structure of the top of the fountain when impinging on an interface. One change which could account for it is illustrated by figures 20(*a*) and 20(*b*) which were taken with a television camera during a repeat of the conditions in figure 15. In the first photograph the fountain touches the interface and it can be seen that the end is smooth, the return flow is narrow and has relatively smooth sides. The second was taken a few minutes later when the fountain height had decreased. The end appears lumpy, the width is larger and there are large eddies along the sides. It appears that when the upward flow impinges on the interface the large eddies are reduced in size. These were not seen in the downward

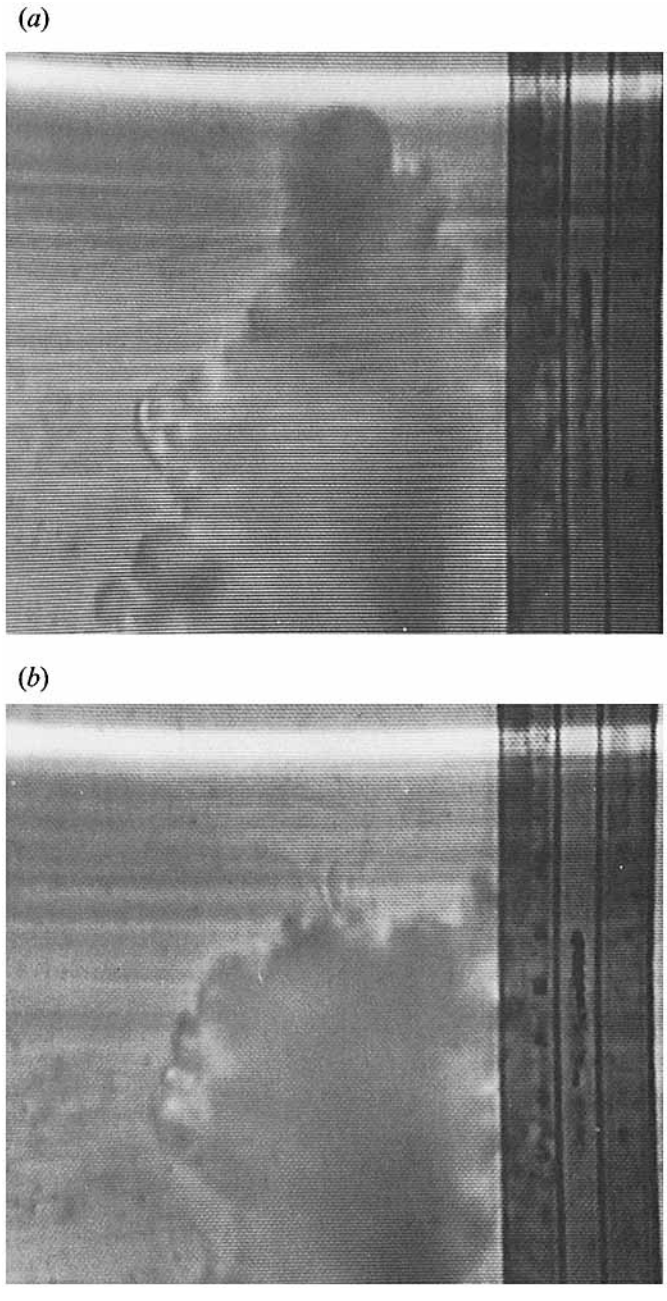

FIGURE 20. Shadowgraphs of the top of a fountain for the conditions of figure 17. (*a*) The top is touching the interface and return flow is narrow. (*b*) The top has dropped back from the interface a few minutes later than (*a*). Return flow is wider and contains larger eddies.

flow. The reason for the elimination of these eddies, which have most of the turbulent energy, must be the very large buoyant forces in the interface which balance the vertical Reynolds stress. Consequently the downward flow does not have large eddies and thus the entrainment is reduced. This should indicate that λ is smaller and the upward

velocity relation, (12), shows that W would be larger at the interface elevation. The fact that the height is greater than the value from (3) is consistent with this deduction.

There are also many weak interfaces seen in these photographs. These must be the result of the observed irregular oscillations of the top of the fountain with a period of many seconds. As these move upward the gradients are intensified and the spacing reduced by the mechanism discussed in §5.1 above. Some were seen to disappear as molecular diffusion smoothed the density profile.

8. Discussion and conclusions

We have presented measurements of the evolution of fountains in an environment which has a forced vertical motion. These and the confirming analyses are extensions of the work on an open container by BTC. We have demonstrated that in all cases the density distribution can be calculated from the conservation equations with the addition of the entrainment function. Several cases have been defined for which the flow is materially different from BTC. These are summarized below.

In the first case the environment velocity opposes the source flow which requires a second inflow at the top of the container. This then develops into a steady flow with an interface and has been used to measure the entrainment to the fountain. This configuration has potential applications in the air conditioning of buildings. If cool air is introduced at low velocity at floor level and a jet of warm air directed down from the ceiling then an interface can be established at a predetermined elevation. The sum of the two inflows would be exhausted at the ceiling and would remove all heat and pollution. A sharp interface could be established which should make for more complete removal of pollutants without mixing.

In the second, the velocity in the zone above the fountain is in the direction of the source flow but of magnitude less than $Q_0 z_r/2A$. This also produces an interface but it is located at the top. The closed container is the limiting case of zero velocity. The interface advances slowly due to entrainment through the top of the fountain. For non-zero velocity the interface advances with the environment particles. The closed-container case covers the heating and cooling of rooms by downward-directed hot jets or upward-directed cold jets. A considerable time is required for the front to reach the opposite surface if the height of the initial fountain is less than the height of the room.

Finally, the environment velocity above the fountain is greater than $Q_0 z_r/2A$. The mean flow is the same as that in the limiting case of the open container and is well described by the analysis developed by BTC. However, for some velocities the top advanced and followed the interface. This produced another interface at a later time. The explanation of this phenomenon may be the change in structure of the end of the fountain upon impinging on an interface.

This study was supported by the Natural Sciences and Engineering Research Council of Canada under grant A-1066. This support is gratefully acknowledged by the authors. The apparatus was constructed by Mr Ernesto Morala who also assisted with some of the experiments. His care and concern are sincerely appreciated.

REFERENCES

BAINES, W. D. 1975 Entrainment by a plume or jet at an interface. *J. Fluid Mech.* **68**, 309–320.

BAINES, W. D. 1983 A technique for the direct measurement of volume flux of a plume. *J. Fluid Mech.* **132**, 247–256.

BAINES, W. D., TURNER, J. S. & CAMPBELL, I. H. 1990 Turbulent fountains in an open container. *J. Fluid Mech.* **212**, 557–592 (referred to herein as BTC).

CRAPPER, P. F. & BAINES, W. D. 1978 Some remarks on non-Boussinesq forced plumes. *Atmos. Environ.* **12**, 1939–1942.

KUMAGAI, M. 1984 Turbulent buoyancy convection from a source in a confined two-layer region. *J. Fluid Mech.* **147**, 105–131.

MORTON, B. R. 1959 Forced plumes. *J. Fluid Mech.* **5**, 151–163.

SEBAN, R. A., BEHNIA, M. M. & ABREAU, K. E. 1978 Temperatures in a heated jet discharged downwards. *Intl J. Heat Mass Transfer* **21**, 1453–1458.

TURNER, J. S. 1966 Jets and plumes with negative or reversing buoyancy. *J. Fluid Mech.* **26**, 779–792.